High-pressure oxidation of the tetragonal La$_{1.5-x}$Ba$_{1.5+x-y}$Ca$_y$Cu$_3$O$_z$ superconductors

J. M. S. Skakle and E. E. Lachowski

Department of Chemistry, University of Aberdeen, Meston Walk, Aberdeen AB24 3UE, Scotland, United Kingdom

R. I. Smith

ISIS, Rutherford Appleton Laboratory, Chilton, Didcot, Oxon, OX11 OQX, United Kingdom

A. R. West

Department of Chemistry, University of Aberdeen, Meston Walk, Aberdeen AB24 3UE, Scotland, United Kingdom

The oxygen content, z, of tetragonal, Ca-doped La$_{1.5}$Ba$_{1.5}$Cu$_3$O$_z$ (La336) superconductors can be increased to values significantly greater than 7.0 by annealing in high-pressure O$_2$. For instance, for La$_{1.1}$Ba$_{1.5}$Ca$_{0.4}$Cu$_3$O$_z$, $z = 7.25$ after heating at 400 °C in 350 bars O$_2$. This contrasts with the behavior of YBa$_2$Cu$_3$O$_z$, which decomposes on attempting to increase z greater than 7.0. The critical temperature, T_c, passes through a maximum of 79 K at an average Cu valence of 2.3–2.4 and decreases to as low as 35 K in the overdoped region of higher Cu valence. T_c data for a range of Ca-doped compositions fall approximately on a single dome-shaped master plot. The crystal structure of LaBa$_{1.5}$Ca$_{0.5}$Cu$_3$O$_z$ shows a complex A-site distribution; in the as-prepared sample, Ca substitutes onto La sites with displacement of La onto Ba sites. After high-pressure treatment, however, Ca substitutes onto Ba sites and La sites are fully occupied by La. The change in A-site distribution appears not to correlate with the maximum in T_c, nor to influence the value of T_c. This behavior of Ca-doped materials is different from that of La$_{1.5}$Ba$_{1.5}$Cu$_3$O$_z$, which cannot be made superconducting even though its nominal Cu valence can be increased sufficiently, and of LaBa$_2$Cu$_3$O$_z$, which has a significantly higher maximum T_c of 94 K and shows an orthorhombic to tetragonal transition with decreasing z. [S0163-1829(97)06518-1]

INTRODUCTION

The structure and properties of YBCO or 123, YBa$_2$Cu$_3$O$_z$ are well known; it has an oxygen-deficient triple-perovskite structure, with an oxygen content, z, variable between 6 and 7. At an oxygen content of 7, it is orthorhombic and superconducting, with a critical temperature, T_c, of 93 K. As oxygen is removed, T_c decreases and the structure changes from orthorhombic to tetragonal at $z \approx 6.5$; at oxygen contents close to this value, YBCO becomes semiconducting. Although, in principle, the YBCO structure contains a large number of oxygen vacancies, two per formula unit, attempts to increase the oxygen content greater than 7 have largely been unsuccessful. Instead, YBCO decomposes to give the 124 phase, YBa$_2$Cu$_4$O$_z$.[1]

YBCO is cation stoichiometric in that the cation ratios are usually regarded as being fixed. With larger rare earth, R, cations in place of Y, the R:Ba ratio is variable and there is a trend towards preferred stabilization of the 336 stoichiometry, typified by La$_{1.5}$Ba$_{1.5}$Cu$_3$O$_z$, at the expense of the 123 stoichiometry, which is difficult to prepare phase pure for $R = $La, Nd.[2–5]

The structure of La336 is perhaps less well known, although it is closely related to that of YBCO.[6] La336 is isostructural with tetragonal YBCO; La occupies the central A-site position, and Ba, La are disordered over the two other A sites. The oxygens are disordered over the $\frac{1}{2}$00, 0$\frac{1}{2}$0 sites in the basal plane, giving tetragonal symmetry at all oxygen contents. La336 is, however, semiconducting at all values of z.[2,7,8] The reason for the absence of superconductivity is not

known; for $z = 7$, the average Cu valence is calculated to be 2.17, well short of the value of ≈ 2.33 often regarded as the optimum for superconductivity in YBCO-type materials. However, a range of oxygen contents, some $\geqslant 7$, have been claimed for La336 but no superconductivity has ever been detected.

To increase the average Cu valence in a 123 or 336 structure, it is clearly necessary to introduce holes. This can be achieved either by increasing the oxygen content or by doping with a lower valent cation. In our earlier studies on La336, Ca and Sr were chosen as feasible substitutes for trivalent La since they are of similar size but divalent.[9–11] In the as-prepared samples, extensive solid solution areas that are superconducting form in both systems; to a first approximation, T_c rises with increasing dopant level, but since the oxygen contents also vary, the detailed behavior is more complex. In these two systems, the highest T_c was 78 K for the composition LaBa$_{1.5}$Ca$_{0.5}$Cu$_3$O$_{7.011}$, which corresponds to an average Cu valence of 2.33.[9,11] The distribution of La, Ba, and Ca over the A sites was found to be more complicated than expected; instead of a simple partial substitution of Ba by Ca, Ca substitutes onto the La sites with concomitant displacement of La onto Ba sites.[11]

Unlike the case of YBCO, the La336 solid solutions do not decompose readily at high oxygen pressures and we have recently shown that instead, the oxygen content of one Ca-doped composition, La$_{1.1}$Ba$_{1.5}$Ca$_{0.4}$Cu$_3$O$_z$, can be increased to $z = 7.25$ after treatment at 350 bars O$_2$ and 400 °C.[12] A direct consequence of this is that the Cu valence increases
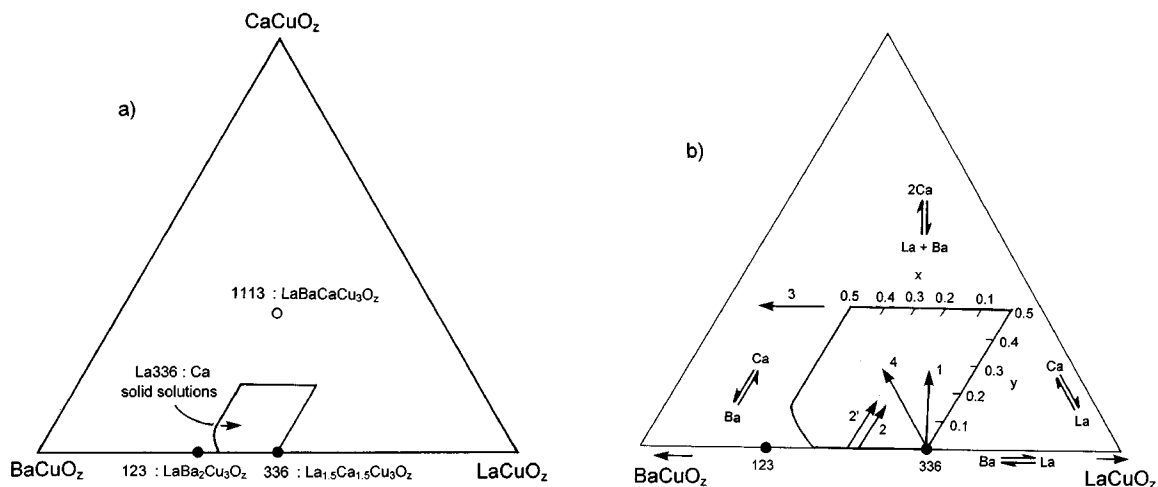
FIG. 1. (a) Location of phases and solid solutions in the pseudoternary phase diagram. (b) La336 solid solution area, compositional grid based on the formula $La_{1.5-x}Ba_{1.5+x-y}Ca_yCu_3O_z$ and possible substitution mechanisms.

well beyond 2.33, the sample becomes overdoped and T_c decreases.

Examples of overdoping of YBCO are known, but these are not associated with oxygen contents, $z > 7$. Thus YBCO itself is regarded as being slightly overdoped at $z = 7$ and the optimum oxygen content is nearer to $z = 6.95$.[13] On aliovalent substitution of Y by Ca, with compensating hole creation, the T_c maximum occurs at lower oxygen contents, e.g., at 84 K and $z = 6.85$ for $Y_{0.8}Ca_{0.2}Ba_2Cu_3O_z$. In several respects, therefore, the La336-based materials behave differently to YBCO. Here, we report a more extensive study of their overdoping at high oxygen contents.

The La336:Ca solid solutions are located on the pseudoternary phase diagram $LaCuO_z$-$BaCuO_z$-$CaCuO_z$, as shown in Fig. 1.[9] They have general formula $La_{1.5-x}Ba_{1.5+x-y}Ca_yCu_3O_z$. With reaction conditions involving heating in air at ~ 950 °C, the solid solutions form for all x and y in the ranges $0 < x, y < 0.5$, apart from those in the corner close to the La123 stoichiometry with $x = 0.5$, $y = 0$. La123 can, by contrast, be prepared by reaction in low partial pressures of O_2,[14] although under these conditions, the La336:Ca solid solutions are not stable.

Numerous other studies on Ca-doped La123-La336 materials have been reported. With the exception of one study in which a solid solution area was identified but not fully characterized,[15] these studies have generally focused on specific substitution mechanisms. Although not explicitly treated as such, these mechanisms can be rationalized and represented in terms of the phase diagram, as shown in Fig. 1(b). Some of these studies started from La336; thus, direction 1 considers compositions on the line between La336 and $CaCuO_2$, in which the most likely solid solution mechanism would be La+Ba=2Ca.[16–18] Direction 2 starts with the stoichiometry La347 (i.e., $x = 0.43$, $y = 0$) to which the partial substitution Ba=Ca is made.[19] Direction 2' is parallel to direction 2 but starts with the composition La5712 (i.e., $x = 0.50$, $y = 0$).[20–27] Direction 3 commences with the composition La3216 (i.e., $x = 0$, $y = 0.5$) and involves the partial substitution La=Ba.[28] Direction 4 commences with La336 and involves the partial substitution La=Ca.[17] Each of these substitutions is perfectly valid but gives only a limited pic-

ture of the doping range and mechanisms possible.

In general, there is good agreement between the various studies as to the solid solution limits. One exception concerns the La1113 composition. In spite of early claims for the existence of a pure phase at this composition, these have not been substantiated in more recent work and, instead, a multiphase assembly forms at this composition.

EXPERIMENTAL

Starting materials were La_2O_3 (Aldrich, 99.99%), $CaCO_3$ (Aldrich, 99.99%), $BaCO_3$ (Aldrich, 99.9%), and CuO (BDH, 99.5%). The La_2O_3 was dried at 1000 °C prior to use, the CuO at 700 °C and the carbonates at 200 °C. Samples were prepared by solid state reaction of appropriate quantities of starting materials and reacted at temperatures between 950 °C and 980 °C. Phase identification was carried out using a Hagg Guinier camera with Cu $K\alpha_1$ radiation. Oxygen contents were determined by reduction in 10% H_2/N_2 on a Stanton Redcroft STA1500 simultaneous TG-DTA instrument, as described in Ref. 11. The average copper valence is determined from the relation: average Cu valence $= 1/3(2Q - z)$ where Q is the total charge on the A sites ($La_{1.5-x}Ba_{1.5+x-y}Ca_y$) and z is the oxygen content. ac susceptibility measurements were carried out on powder samples using a Lakeshore AC7000 susceptometer: $f = 666$ Hz; $H = 2$ A m^{-1}. Data for accurate unit cell determination were collected on a Stoe Stadi/P diffractometer in transmission mode using a small linear position sensitive detector of resolution 0.02° 2θ, with Cu $K\alpha_1$ radiation ($\lambda = 1.540\,56$ Å, Ge monochromator). Unit cells were refined using the Stoe lattice refinement package, LATREF.

Samples were annealed under high pressures of oxygen at 400 °C using a Morris Research Inc. high oxygen pressure furnace, Model No. HPS5015E7. Pellets were prepared, wrapped in gold foil, and placed in an alumina boat; starting pressures of 25–200 bars were employed, giving pressures at 400 °C of 50–400 bars. At the end of each run, samples were cooled slowly to ambient temperature whilst still under pressure, removed and analyzed using a range of techniques.

For neutron diffraction, 5–10 g samples were prepared as

above. Samples were placed in cylindrical V cans and data collected on the POLARIS diffractometer at the UK Spallation neutron source, ISIS at Rutherford Appleton Laboratory. The crystal structures were refined by the Rietveld method using the program TF14LS,[29,30] using data collected over the time-of-flight range 2000–19500 μs using the highest resolution, backscattering detectors. Scattering lengths were taken from Sears.[31]

The homogeneity of the high-pressure-annealed samples was checked by electron probe microanalysis (EPMA) using a Cameca SX51 EPMA. Transmission electron microscopy (TEM) and selected area electron diffraction (SAED) were performed on a JEOL TEMSCAN instrument.

RESULTS

Ten samples were prepared with compositions, given by the general formula $La_{1.5-x}Ba_{1.5+x-y}Ca_yCu_3O_z$, in the range $0 \leq x \leq 0.5$, $0 \leq y \leq 0.5$, Table I, as described previously[9,11] and confirmed to be phase pure by x-ray powder diffraction, in agreement with the phase diagram.[9] The samples fall into two groups, those with the nominal replacement La=Ca, i.e., with $x=y$ in the general formula, and those with the replacement Ba=Ca, i.e., with $x=0$ and varying y. These samples were then divided into several portions and heated in a range of oxygen pressures at 400 °C. All samples were subsequently analyzed by thermogravimetry (to obtain z, using methods described in Ref. 9), ac susceptometry (to obtain T_c) and x-ray powder diffraction (to check phase purity). Results are summarized in Table I. Some samples were additionally examined by EPMA (to confirm phase purity and perform elemental analysis), TEM (to confirm unit cell symmetry and look for the possible presence of supercell formation), and x-ray and neutron powder diffraction (for lattice parameters and Rietveld refinement). Results for the latter are given in Table II.

The oxygen content as a function of annealing pressure for one composition, $x=y=0.4$, and for pressures between 0.21 and 350 bar O$_2$ is shown in Fig. 2. These data are typical of all compositions studied in that z increases with pressure, without any indication of reaching a pressure-independent limit; see Table I. The data are approximately linear over the range 1–350 bars O$_2$. We have not studied oxygen contents at subambient pressures but note that the oxygen contents in 1 bar air and O$_2$ differ significantly. It is possible, therefore, that a second regime of pressure dependence occurs for pressures below about 1 bar O$_2$. We note also that the region 1–50 bars corresponds to a crystallographic change in the A-site distribution (see later) and to a discontinuity in lattice parameters (Fig. 7; see later) Further work is required to establish whether two regions of pressure dependence do, in fact, occur and whether these are linked to different A-site arrangements.

For the same composition and samples, T_c is plotted against z in Fig. 3. The plot clearly passes through a maximum at $z \approx 7.05$, corresponding to an average Cu valence of 2.33. It is notable that for this composition, $x=y=0.4$, T_c is not optimized in samples annealed under 1 bar oxygen; on high-pressure annealing, T_c first increases to a maximum of 79 K, then falls as low as 35 K upon annealing at 350 bars.

Data for the other nine compositions studied were ana-

TABLE I. Oxygen contents and T_c values for high-pressure-annealed samples.

$x=y$	Sample	T_c (K)	Oxygen content	Average Cu valence
0.5	Air	40	6.790	2.193
0.5	Oxygen	78	7.011	2.341
0.5	50 bars	76	7.079	2.386
0.5	75 bars	72	7.112	2.408
0.5	125 bars	56	7.160	2.440
0.4	Air	34	6.76	2.14
0.4	Oxygen	70	6.97	2.28
0.4	25 bars	79	7.06	2.34
0.4	50 bars	79	7.06	2.34
0.4	75 bars	77	7.11	2.373
0.4	100 bars	76	7.123	2.382
0.4	125 bars	70	7.17	2.413
0.4	175 bars	35	7.25	2.467
0.3	Air	27	6.72	2.08
0.3	Oxygen	60	6.93	2.22
0.3	75 bars	75.2	7.06	2.307
0.2	Air	20	6.70	2.03
0.2	Oxygen	45	6.92	2.18
0.2	75 brs	52	6.94	2.193
0.1	Air		6.688	1.992
0.1	Oxygen	25	6.903)	2.135
0.1	75 bars	40	6.943	2.162
0.1	125 bars	51	6.982	2.188
0.0	Air		6.657	1.938
0.0	Oxygen		6.884	2.090
0.0	75 bars		7.021	2.180
0.0	125 bars		7.078	2.220
0.0, 0.1	Air	11	6.888	2.092
0.0, 0.1	Oxygen	16	6.912	2.108
0.0, 0.1	75 bars	25	6.932	2.121
0.0, 0.1	125 bars	35	6.964	2.143
0.0, 0.2	Air	16	6.897	2.098
0.0, 0.2	Oxygen	25	6.918	2.112
0.0, 0.2	75 bars	32	6.957	2.138
0.0, 0.2	125 bars	42	7.002	2.168
0.0, 0.4	Air	25	6.764	2.009
0.0, 0.4	Oxygen	40	6.969	2.146
0.0, 0.4	75 bars	55	7.050	2.200
0.0, 0.4	125 bars	62	7.082	2.221
0.0, 0.5	Air	30	6.801	2.034
0.0, 0.5	Oxygen	50	6.981	2.154
0.0, 0.5	75 bars	67	7.126	2.251
0.0, 0.5	125 bars	74	7.195	2.297

lyzed similarly; see Table I; all the data are collected onto a master diagram in Fig. 4, apart from those for the undoped composition, $x=y=0$, which was found to be semiconducting under all conditions and whose behavior is totally anomalous in comparison with that of the doped samples.

TABLE II. Refined structural parameters for $LaBa_{1.5}Ca_{0.5}Cu_3O_z$ from neutron diffraction data. [In the final refinement, the Ba/Ca and La site occupancies were fixed as 0.75:0.25 and 1.00, respectively, as in the text. These occupancies were deduced from earlier refinements in which the isotropic temperature factors, ITF, were held constant and the site occupancies refined. In all cases, there was no evidence for Ca occupying the La site and the Ba:Ca ratio refined to within 2 e.s.d's of 0.75:0.25 (where one e.s.d.$=\pm 0.01$).]

Sample	HPO25	HPO50	HPO100	HPO150	HPO200	Pretreated	
Pressure (bar)	50	100	200	300	400	Ambient	
Oxygen content	7.10	7.12	7.14	7.16	7.18	7.02(2)	
a (Å)	3.88098(3)	3.88025(2)	3.88001(3)	3.87898(2)	3.87873(2)	3.88485(2)	a (Å)
c (Å)	11.71047(11)	11.70377(13)	11.70345(12)	11.70319(12)	11.69815(9)	11.74001(9)	c (Å)
Ba/Ca z	0.1831(1)	0.1831(1)	0.1828(1)	0.1828(1)	0.1827(1)	0.1898(1)	Ba/Ca z
Cu(2) z	0.34881(8)	0.34871(9)	0.34866(8)	0.34856(9)	0.34855(8)	0.35168(8)	Cu(2) z
O(2) z	0.36478(8)	0.36474(8)	0.36468(9)	0.36464(8)	0.36454(8)	0.36509(9)	O(2) z
O(3) z	0.1573(2)	0.1573(2)	0.1571(2)	0.1571(2)	0.1571(2)	0.1538(2)	O(3) z
La ITF	0.58(2)	0.59(2)	0.60(2)	0.62(2)	0.62(2)	0.53(2)	La ITF
Ba/Ca ITF	0.62(2)	0.63(2)	0.62(2)	0.63(2)	0.61(2)	0.83(2)	Ba/Ca ITF
Cu(1) ITF	1.00(2)	1.00(3)	1.04(2)	1.00(3)	1.00(2)	1.21(2)	Cu(1) ITF
Cu(2) ITF	0.27(1)	0.27(1)	0.28(1)	0.28(1)	0.28(1)	0.30(1)	Cu(2) ITF
Cu(1)-O(1)	1.9405	1.9401	1.9400	1.9395	1.9394	1.9424	Cu(1)-O(1)
Cu(1)-O(3)	1.8421	1.8410	1.8386	1.8386	1.8378	1.8056	Cu(1)-O(3)
Cu(2)-O(2)	1.9495	1.9492	1.9490	1.9486	1.9484	1.9488	Cu(2)-O(2)
Cu(2)-O(3)	2.2427	2.2402	2.2419	2.2407	2.2396	2.3231	Cu(2)-O(3)

The data in Fig. 4 demonstrate a universal pattern of behavior for the Ca-doped compositions of this series, independent of cation stoichiometry and with average Cu valence, given by the oxygen content, as the main variable; the data pass through a maximum at ca. 79 K for a Cu valence between 2.3 and 2.4 and drop sharply in the region of overdoping. Although all T_c data fall onto a single master curve, the T_c maximum occurs at different oxygen contents for different values of x. This is because, with decreasing values of x, the average Cu valence decreases for a given oxygen content. Hence T_c(max) occurs at increasing values of z for decreasing values of x.

Electron diffraction patterns for the composition $x=y=0.5$, $z=7.20$ are shown in Fig. 5; reflections form a square lattice, consistent with the expected tetragonal symmetry and show no evidence of supercell formation. A lattice image is shown in Fig. 6 and clearly indicates the periodicity (~ 12 A) along the c axis, with no evidence of intergrowths. Previously, we had shown the Ca-doped La336 materials to
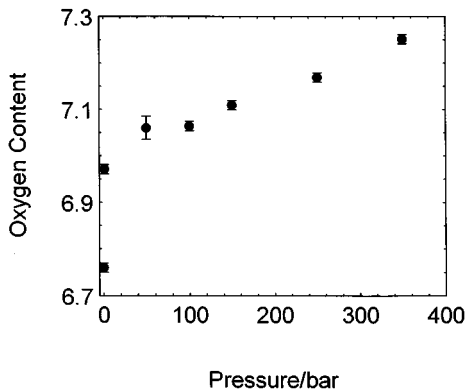
be tetragonal after heating at ambient pressure; the present results show that high-pressure treatment has no noticeable effect on the basic structure.

The variation of unit cell parameters, **a** and **c**, with annealing pressure for a range of compositions x and y is shown in Fig. 7(a); **a** is largely insensitive to pressure and oxygen content but **c** decreases significantly, especially at lower pressures. This decrease is smallest for the undoped 336 composition $x=y=0$. The variation of cell parameters with oxygen content is shown for one composition, $x=y=0.4$ in Fig. 7(b); all other Ca-doped compositions behaved similarly. The variation with oxygen content is markedly nonlinear. Relatively small changes are seen for oxygen con-
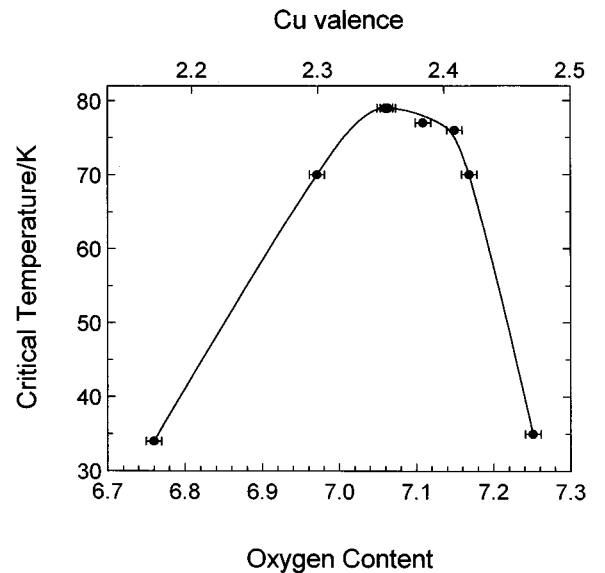

FIG. 2. Oxygen content of composition $x=y=0.4$ as a function of oxygen pressure.

FIG. 3. Critical temperature as a function of oxygen content and average Cu valence for $x=y=0.4$. Same data as for Fig. 2.
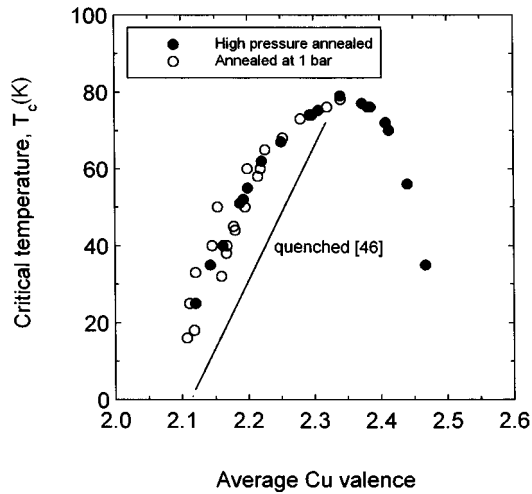
FIG. 4. Master plot of T_c vs average Cu valence for all Ca-doped samples together with linear dependence observed in quenched samples.

tents below about 7. Between 7 and 7.05, a rapid decrease occurs, especially in **c**; at higher oxygen contents the cell parameters again decrease more gradually. A smooth variation of the unit cell parameters with oxygen content might be expected; it is likely, therefore, that some additional struc-

tural changes other than simple intercalation of oxygen into the basal sites may cause the anomalous decrease in the unit cell parameters.

The exception to the above pattern of behavior is shown by the undoped composition $x=y=0.0$, $La_{1.5}Ba_{1.5}Cu_3O_z$, in which the lattice parameters show a simple smooth change with annealing pressure and hence with oxygen content; see Fig. 7(c). For this composition, it would seem that the addition of oxygen, causing the oxidation of Cu and concomitant decrease in the unit cell dimensions, is the only change that occurs on high-pressure annealing and that there are no additional structural changes at intermediate oxygen contents.

In order to investigate possible structural changes, high-pressure-annealed samples of composition $x=y=0.5$, together with samples prepared at ambient pressure were studied by neutron diffraction. In all cases, both La and Ca were placed on both sets of A sites initially, to give $(La_{0.75}Ca_{0.25})(Ba_{1.5}La_{0.25}Ca_{0.25})Cu_3O_z$, and the cation site occupancies were refined within the overall constraint that the cation stoichiometry was fixed at the nominal value of $LaBa_{1.5}Ca_{0.5}$. The unit cell dimensions obtained from the refinements are shown in Fig. 8, for samples annealed at both ambient (open circles) and high pressures (solid squares) of oxygen. Again, there is a marked discontinuity in the size of the unit cell dimensions between the samples treated at high and ambient pressures, similar to that shown in Fig. 7 for the x-ray diffraction analyses.
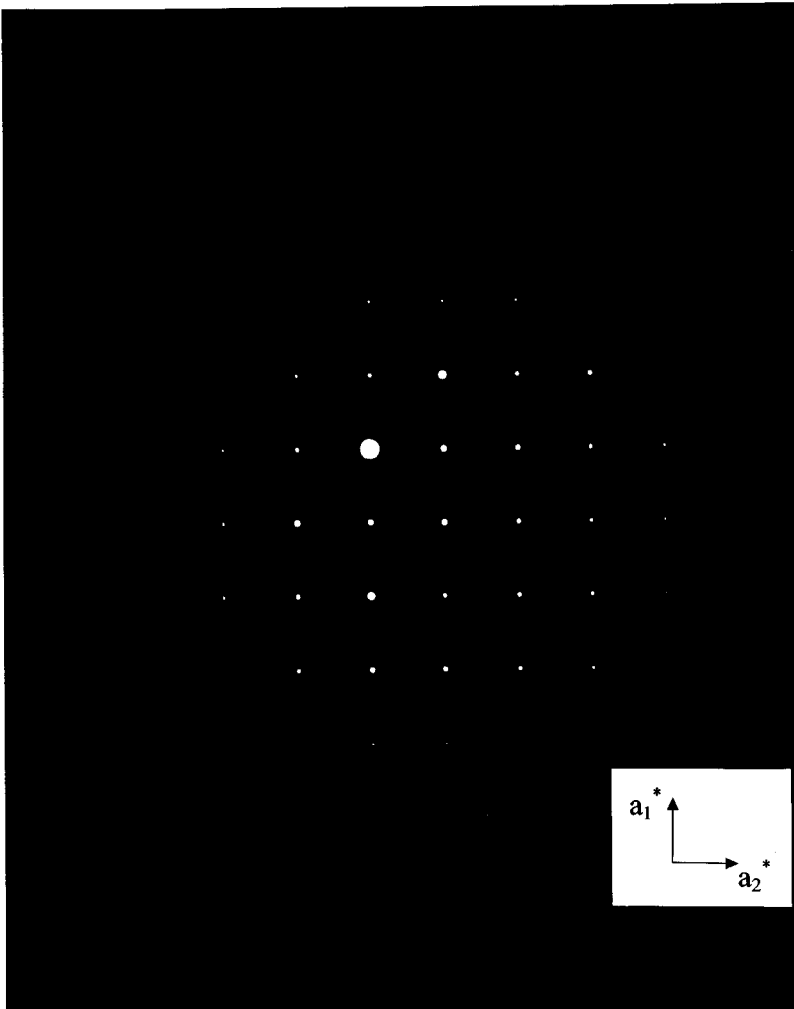

FIG. 5. Electron diffraction pattern: $hk0$ section of the reciprocal lattice for composition $x=y=0.4$ after heating at 350 bars O_2.

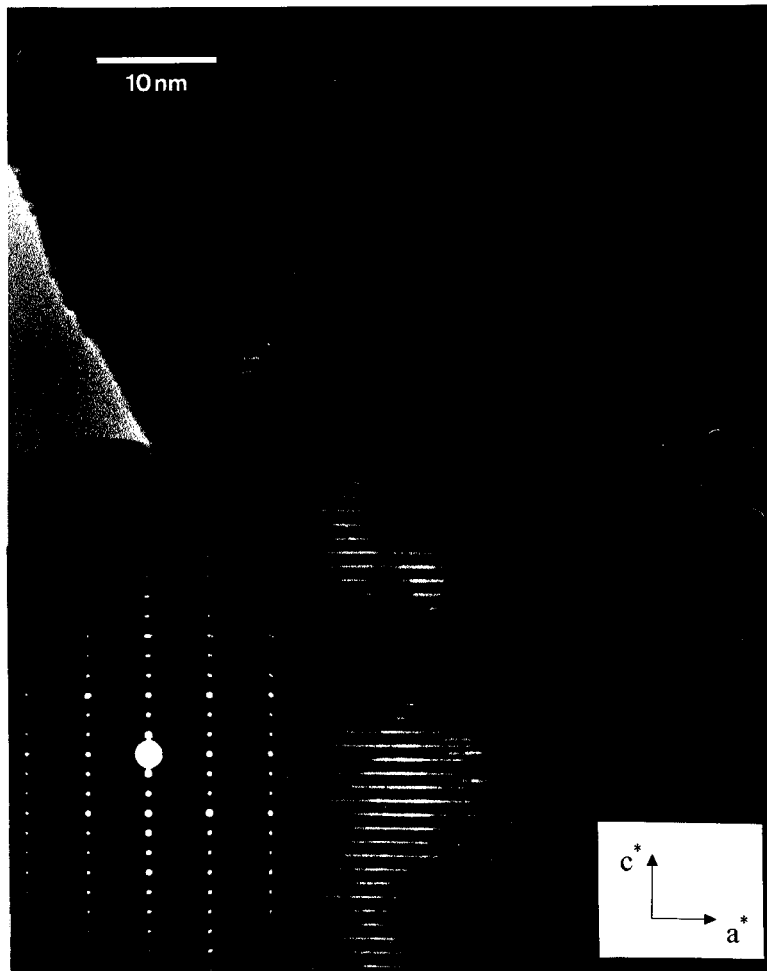FIG. 6. Electron diffraction pattern:$h01$ section and corresponding lattice image for the same sample as in Fig. 5.
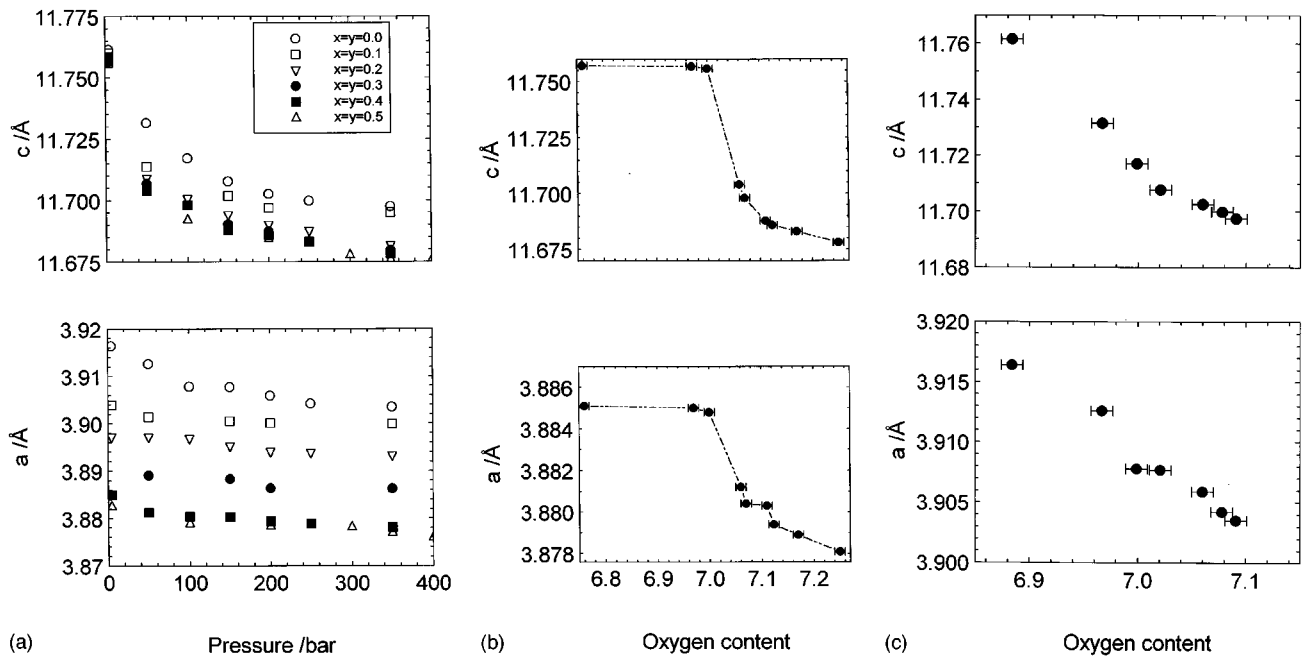

FIG. 7. (a) Lattice parameters obtained at room temperature and pressure vs pressure used for high-pressure oxygen anneals for a range of Ca-doped samples. (b) As in (a), lattice parameters vs oxygen content for composition $x=y=0.5$ ($LaBa_{1.5}Ca_{0.5}Cu_3O_z$); x-ray diffraction analysis. (c) As in (a), lattice parameters vs oxygen content for composition $x=y=0.0$ ($La_{1.5}Ba_{1.5}Cu_3O_z$).
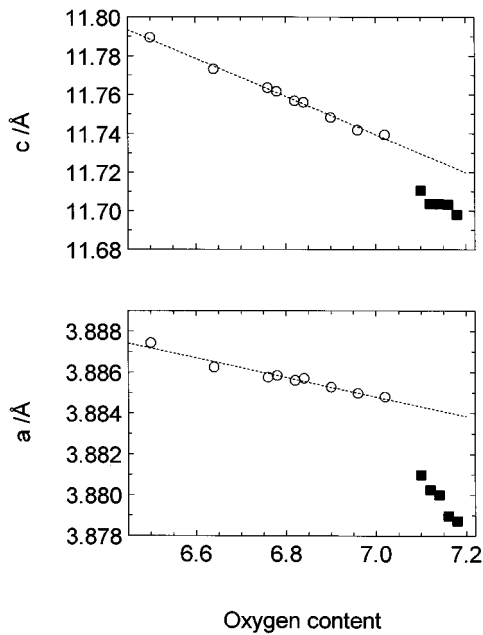
FIG. 8. As in Fig. 7(a), lattice parameters vs oxygen content for composition $x=y=0.5$; neutron diffraction analysis.

The cation site occupancies obtained from the Rietveld refinement, Table II, also fall into two sets. For the samples annealed at ambient pressure, Ca was found to occupy the La site with concomitant displacement of La onto the Ba site to give the formula

$$(La_{0.5}Ca_{0.5})(Ba_{1.5}La_{0.5})Cu_3O_z .$$
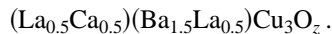
This is in agreement with our earlier results obtained from x-ray powder diffraction data.[11] In the high-pressure-annealed samples, however, Ca was found to occupy the Ba site, to give the formula

$$(La)(Ba_{1.5}Ca_{0.5})Cu_3O_z .$$

This structural change appears to correlate with the anomaly in the unit cell parameters at $z=7.00-7.05$; see Figs. 7 and 8.
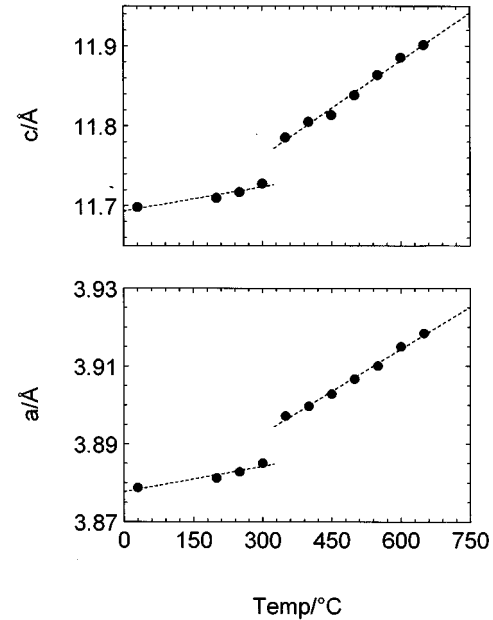

FIG. 9. Lattice parameters obtained as a function of temperature for composition $x=y=0.5$ after high-pressure oxygenation; sample heated under vacuum.

To test the stability of the high-pressure form of the La-BCCO structure, a sample prepared under 350 bars of oxygen, $x=y=0.5$, $z=7.18$, was heated to 650 °C under vacuum in a furnace at the Rutherford Appleton Laboratory and neutron diffraction data collected *in situ* as a function of temperature. Data sets were collected at 50 °C intervals and the structure refined as before. Results are summarized in Table III. Lattice parameters as a function of temperature are shown in Fig. 9. Superposed on a gradual increase in **a** and **c**, there is a discontinuity at 300–350 °C. The lattice parameters, however, are likely to be affected by oxygen content as well as temperature and both vary during this experiment. Oxygen contents, obtained from Rietveld refinement of the high temperature data are shown as a function of temperature in Fig. 10. They are approximately constant to 300 °C, undergo a rapid decrease at 300–350 °C followed by a more gradual, approximately linear decrease up to the highest tem-

TABLE III. Refined parameters as a function of temperature (under vacuum) for high-pressure-annealed samples of LaBa$_{1.5}$Ca$_{0.5}$Cu$_3$O$_z$.

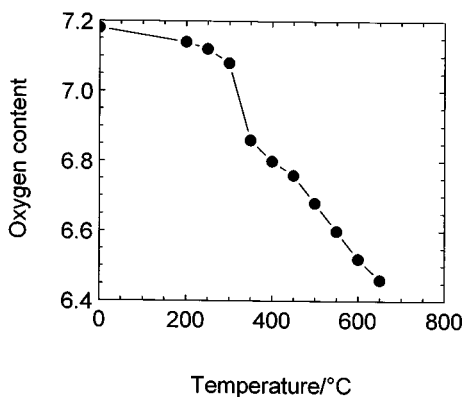| $T/°C$	200	250	300	350	400	450	500	550	600	650
a (Å)	3.88122(3)	3.88281(3)	3.88508(3)	3.89722(3)	3.89975(3)	3.90288(4)	3.90668(4)	3.91003(4)	3.91499(4)	3.91838(4)
c (Å)	11.7098(1)	11.7170(1)	11.7278(1)	11.7858(1)	11.8052(1)	11.8136(1)	11.8384(1)	11.8637(1)	11.8855(1)	11.9013(1)
Ba/Ca z	0.1832(2)	0.1834(2)	0.1840(2)	0.1869(2)	0.1877(2)	0.1882(2)	0.1898(2)	0.1905(2)	0.1916(2)	0.1921(2)
Cu2 z	0.3488(1)	0.3490(1)	0.3493(1)	0.3506(1)	0.3510(1)	0.3512(1)	0.3518(1)	0.3522(1)	0.3527(1)	0.3530(1)
O2 z	0.3646(1)	0.3646(1)	0.3647(1)	0.3651(1)	0.3652(1)	0.3653(1)	0.3654(1)	0.3655(1)	0.3657(1)	0.3658(1)
O3 z	0.1568(2)	0.1568(2)	0.1564(2)	0.1548(2)	0.1543(2)	0.1540(2)	0.1534(2)	0.1530(2)	0.1525(2)	0.1522(2)
O1 SITE	0.57(1)	0.56(1)	0.54(1)	0.43(1)	0.40(1)	0.38(1)	0.34(1)	0.30(1)	0.26(1)	0.23(1)
Oxygen	7.14	7.12	7.08	6.86	6.80	6.76	6.68	6.60	6.52	6.46
La ITF	0.84(2)	0.92(2)	1.00(2)	1.09(2)	1.21(2)	1.31(3)	1.30(3)	1.44(3)	1.51(3)	1.59(3)
Ba/Ca ITF	0.83(2)	0.90(3)	0.97(3)	1.07(3)	1.24(3)	1.32(4)	1.36(4)	1.42(4)	1.50(4)	1.57(4)
Cu1 ITF	1.22(3)	1.18(3)	1.36(3)	1.45(3)	1.70(4)	1.89(4)	2.03(4)	2.24(4)	2.46(5)	2.61(5)
Cu2 ITF	0.47(1)	0.53(1)	0.59(2)	0.64(2)	0.68(2)	0.74(2)	0.76(2)	0.81(2)	0.86(2)	0.89(2)

FIG. 10. Oxygen content vs temperature for the sample and data used in Fig. 9. The variation in oxygen content was achieved by heating the sample under vacuum and was determined from site occupancies obtained by Rietveld refinement of the high temperature neutron diffraction data.

perature studied, 650 °C. The loss of oxygen below 350 °C corresponds to that gained during the high-pressure-annealing treatment.

The results of Figs. 9 and 10 are combined in Fig. 11 to give lattice parameters as a function of oxygen content. Data are essentially linear for both **a** and **c**; the unit cell contracts as oxygen is intercalated into the structure, consistent with the increased average oxidation state of Cu leading to stronger, shorter Cu-O bonds. It should be remembered that the data shown in Fig. 11 also have temperature as a variable; since the crystal structure presumably expands with temperature, any expansion effects are superposed on the variation with oxygen content. Nevertheless, assuming a typical expansion coefficient of 1×10^{-5} °C^{-1}, the changes shown in Fig. 11 are three orders of magnitude larger. It can be con-
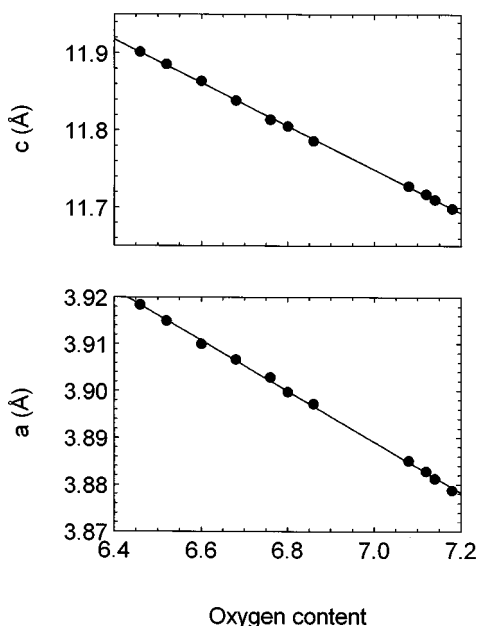
cluded, therefore, that the data shown in Fig. 11 are largely uninfluenced by thermal expansion effects.

The Rietveld refinement results showed that the occupancy of the A sites was essentially unchanged on heating, i.e., that Ca partially occupied the Ba sites. Thus, for this composition at least, it is possible to prepare materials with a range of oxygen contents but with different A-site distributions: in the high-pressure treated sample and after heating subsequently, in vacuum, at temperatures up to 650 °C, Ca occupies the Ba sites whereas in the originally prepared sample which was not subjected to high-pressure oxygenation, the alternative A site distribution (Ca$_{La}$+La$_{Ba}$, i.e., Ca occupies the La sites and La occupies the Ba sites), was found.

From the Rietveld refinement results, Table III, bond length data involving Cu were extracted and are plotted against oxygen content in Fig. 12. In all cases, the Cu-O and Cu-Cu bonds show a linear variation with z. Again, the data were obtained at different temperatures, but the effects of thermal expansion are negligible in comparison with the effect of varying oxygen content, z.

For other compositions within the solid solution area, it has not yet been possible to use neutron diffraction to investigate the cation distributions. Figure 7 shows the variation of lattice parameters as determined by x-ray diffraction with annealing pressure, (a), and for one composition, with oxygen content (b); the lattice parameters of all compositions, apart from $x=y=0$. showed a marked drop upon annealing under pressure. It is implied, therefore, that the structural changes found in LaBa$_{1.5}$Ca$_{0.5}$Cu$_3$O$_z$ ($x=y=0.5$) on high pressure treatment are also responsible for a similar anomalous change in lattice parameters of the other doped compositions. The behavior of the undoped composition $x=y=0$ is different; it shows little sign of any anomaly in lattice parameters, Fig. 7(c). No transition in A-site distribution is anticipated, therefore, consistent with the fact that this composition contains no Ca^{2+} ions.

DISCUSSION

The results obtained by high-pressure annealing show that the oxygen content of La336:Ca solid solutions can be increased by treatment at low temperatures (400 °C); the maximum achieved was 7.25 using a pressure of 350 bars. The graph of oxygen content versus pressure did not reach a plateau, indicating that higher values of oxygen content could be achieved under higher pressures; there is no indication of any decomposition at high oxygen pressures, such as occurs with Y123. In theory, because the 123-336 type structure is an oxygen-deficient triple perovskite, it should be possible to increase the oxygen content to 9.

By increasing the oxygen content of the La336:Ca solid solutions, the overdoped region of the system has been accessed; the maximum in T_c is clearly shown. Similar behavior is well known for systems such as La$_{2-x}$Ba$_x$CuO$_4$ and the BiSCCO's; it has not been demonstrated clearly before in these structures although it has been suggested as a possibility for La123.[32] In Y123, overdoping was achieved only by aliovalent doping (e.g., Ca^{2+} substituting for Y^{3+}) (see, e.g., Refs. 13, 33, and 34); it has not been possible to overdope Y123 by increasing the oxygen content.

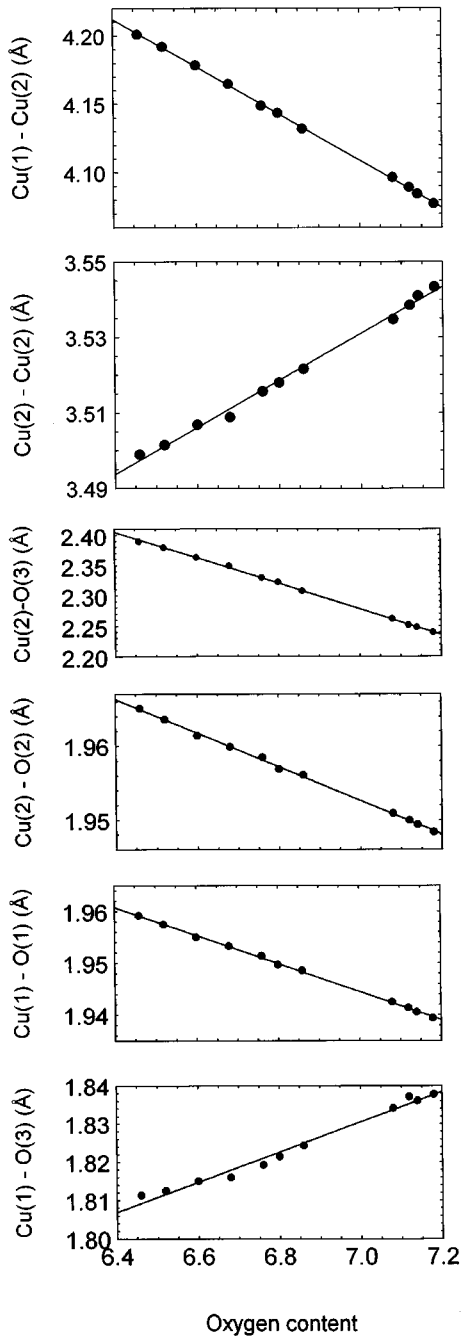FIG. 11. Lattice parameters vs oxygen content; data obtained from Figs. 9 and 10.

FIG. 12. Selected bond lengths vs oxygen content for composition $x=y=0.5$.

The curve of critical temperature vs Cu valence appears to be universal for doped samples in the $La_{1.5-x}Ba_{1.5+x-y}Ca_yCu_3O_z$ system, see Fig. 4. The "336" phase does not, however, fit the general trend. Despite an earlier report of a T_c of 15 K;[35] it appears to be well established that $La_{1.5}Ba_{1.5}Cu_3O_z$ is semiconducting. One reason suggested was that the Cu valence is too low for superconductivity. However, if we were to regard the T_c vs Cu valence curve as universal for the $La_{1.5-x}Ba_{1.5+x-y}Ca_yCu_3O_z$ system, then $La_{1.5}Ba_{1.5}Cu_3O_{7.08}$ (Cu valence=2.22) should have a critical temperature of around 55 K. This was clearly not the case. Samples doped with $\geqslant 10\%$ Ca for Ba do follow the master-curve behavior. $La_{1.5}Ba_{1.5}Cu_3O_z$ is, therefore,

a distinct composition and merits further study as to why it does not exhibit superconductivity. David *et al.* suggest that due to oxygen localizations in samples with oxygen contents greater than 7, superconductivity in 336 is possible only for oxygen stoichiometries less than 7;[6] our studies confirm that no superconductivity is observed in 336 samples with oxygen contents higher than 7, but also have shown no evidence of superconductivity above 4 K for samples with oxygen contents lower than 7.

The A-site cation arrangement of high-pressure-annealed samples differs from that of the as-prepared samples, and is kinetically stable in this arrangement up to at least 650 °C. In the related systems $YBa_2Cu_4O_8$ (124) and $Y_2Ba_4Cu_7O_{15}$ (247), there has been much controversy in the literature as to the substitution mechanism when the dopant ion is Ca. Ca^{2+} is of similar size to Y^{3+}, but the same valence as Ba^{2+} and so may, in theory, substitute to some degree on either site. The most recent neutron diffraction results (e.g., Refs. 36–39) indicate that Ca substitutes on the Y sites of Y-124 prepared at high pressure. Buckley *et al.* prepared samples both at high pressure and at ambient,[34] and for both these conditions Ca was shown to substitute at both sites. Zhang, however, demonstrated that Ca substitution closely mimics the effect of external pressure,[40] and that Ca must substitute on Ba sites; NQR (nuclear quadropole resonance) and EELS results largely suport this deduction.[41–43] Similar ambiguities exist over the substitution of Ca into $Y_2Ba_4Cu_7O_{15}$.[34,36,44] Here, for the composition $LaBa_{1.5}Ca_{0.5}Cu_3O_z$, we have demonstrated that Ca can substitute for either La or Ba, depending on the preparation conditions. It is possible that differing preparative conditions could be responsible for the differing results in the Y-124 and 247 systems.

The existence of a single master curve of T_c vs average Cu valence, Fig. 4, similar to that observed with other cuprate systems,[45] implies that hole concentration is the key parameter controlling T_c for a given structure. In the underdoped region of Fig. 4, however, the data show some scatter which indicates that additional factors influence T_c. In a series of papers[20–27] concerning materials in direction $2'$, Fig. 1, for which the overall A-site cation charge (La+Ba+Ca) is constant at 7.25(+), Goldschmidt *et al.* have shown that a range of T_c values is possible at constant oxygen content. They interpret this as arising from variable degrees of internal charge transfer between the two types of Cu sites in the crystal structure. Additional evidence for the possibility of internal charge transfer, although not explicitly recognized as such, comes from the observation of "double plateau" behavior in the plot of T_c vs oxygen content of a La123:Ca solid solution composition, $x=y=0.5$:[46] materials that were cooled rapidly showed a linear dependence of T_c on oxygen content, whereas slowly cooled samples showed somewhat higher-T_c values and a double plateau dependence on oxygen content.

The data shown in Fig. 4 are for samples that had been cooled to ambient over a period of several hours after high-pressure oxygenation at 400 °C. These are compared with those that were quenched to ambient after annealing at 1 bar in Fig. 4; data on materials quenched after high-pressure oxygenation are not available. This clearly shows that the slowly cooled samples have a higher T_c, by up to 25 K depending on oxygen content, than the rapidly quenched samples. Hence the master curve of T_c vs oxygen content

applies strictly to samples prepared under similar conditions. If the conditions vary, such as using different cooling rates, then departures from the master curve behavior occur.

CONCLUSIONS

The oxygen content of La336:Ca solid solutions can be increased by high-pressure oxygenation, the samples become overdoped and T_c decreases. This behavior contrasts with that of Y 123 which decomposes at high oxygen pressures. The T_c data for a wide range of cation contents fall on a master curve of T_c vs average Cu valence, thus showing that hole concentration is the main factor that controls T_c for materials in this structural family. In the underdoped region, there is some scatter in the experimental T_c data and this is attributed to varying degrees of internal charge transfer which effectively allows the hole concentration to vary without any change in overall composition. For a given composition, the degree of internal charge transfer may vary systematically with temperature and hence, the cooling rate after synthesis is an important variable in controlling the hole concentration and T_c.

ACKNOWLEDGMENTS

[1] K. Conder, J. Karpinski, E. Kaldis, S. Rusiecki, and E. Jilek, Physica C **196**, 164 (1992).

[2] C. U. Segre, B. Dabrowski, D. G. Hinks, K. Zhang, J. D. Jorgensen, M. A. Beno, and I. K. Schuller, Nature **329**, 227 (1987).

[3] T. Wada, N. Suzuki, A. Maeda, T. Yabe, K. Uchinokura, S. Uchida, and S. Tanaka, Phys. Rev. B **39**, 9129 (1989).

[4] K. Zhang, B. Dabrowski, C. U. Segre, D. G. Hinks, I. K. Schuller, J. D. Jorgensen, and M. Slaski, J. Phys. C **20**, L935 (1987).

[5] J. M. S. Skakle and A. R. West, Physica C **261**, 105 (1996).

[6] W. I. F. David, W. T. A. Harrison, R. M. Ibberson, M. T. Weller, J. R. Grasmeder, and P. Lanchester, Nature **328**, 328 (1987).

[7] S. A. Sunshine, L. F. Schneemeyer, J. V. Waszczak, D. W. Murphy, S. Miraglia, A. Santoro, and F. Beech, J. Cryst. Growth **85**, 632 (1987).

[8] C. C. Torardi, E. M. McCarron, M. A. Subramanian, A. W. Sleight, and D. E. Cox, Mater. Res. Bull. **22**, 1563 (1987).

[9] J. M. S. Skakle and A. R. West, Physica C **220**, 187 (1994).

[10] J. M. S. Skakle and A. R. West, Physica C **241**, 191 (1995).

[11] J. M. S. Skakle and A. R. West, Physica C **227**, 336 (1994).

[12] J. M. S. Skakle, A. Coats, and A. R. West (unpublished).

[13] J. L. Tallon and N. E. Flower, Physica C **204**, 237 (1993).

[14] J. M. S. Skakle and A. R. West, J. Mater. Chem. **4**, 1745 (1994).

[15] T. Mertelj, P. Stastny, F. C. Matacotta, P. Ganguly, C. U. Segre, and D. Mihailovic, Physica C **183**, 11 (1991).

[16] S. Engelsberg, Physica C **176**, 451 (1991).

[17] R. A. Gunasekaran, J. V. Yakhmi, and R. M. Iyer, Physica C **208**, 143 (1993).

[18] H-C. I. Kao, Y. D. Leu, W. N. Huang, C-M. Wang, D. H. Chen, and T. J. Lee, Supercond. Sci. Technol. **9**, 893 (1996).

[19] D. S. Wu, Y. F. Yang, H.-C. I. Kao, and C. M. Wang, Physica C **212**, 32 (1993).

[20] D. Goldschmidt, G. M. Reisner, Y. Direktovich, A. Knizhnik, E. Gartstein, G. Kimmel, and Y. Eckstein, Physica C **217**, 217 (1993).

[21] D. Goldschmidt, G. M. Reisner, Y. Direktovitch, A. Knizhnik, E. Gartstein, G. Kimmel, and Y. Eckstein, Phys. Rev. B **48**, 532 (1993).

[22] D. Goldschmidt, Y. Direktovitch, A. Knizhnik, and Y. Eckstein, Phys. Rev. Lett. **71**, 3392 (1993).

[23] D. Goldschmidt, A. Knizhnik, Y. Direktovitch, G. M. Reisner, and Y. Eckstein, Phys. Rev. B **49**, 15 928 (1994).

[24] D. Goldschmidt, Y. Direktovitch, A. Knizhnik, and Y. Eckstein, Phys. Rev. B **51**, 6739 (1995).

[25] D. Goldschmidt, A. Knizhnik, Y. Direktovitch, G. M. Reisner, and Y. Eckstein, Phys. Rev. B **52**, 12 982 (1995).

[26] C. Chabaud, Y. Direktovitch, I. Gertner, G. M. Reisner, A. Knizhnik, D. Goldschmidt, Y. Eckstein, and G. Koren, Physica C **261**, 33 (1996).

[27] D. Goldschmidt, A.-K. Klehe, J. S. Schilling, and Y. Eckstein, Phys. Rev. B **53**, 14 631 (1996).

[28] V. P. Sirotinkin, O. I. Eshniyazov, D. R. Tursunova, A. A. Evdokimov, and P. A. Arsen'ev, Russ. J. Inorg. Chem. **35**, 1706 (1990).

[29] R. I. Smith and S. Hull (unpublished).

[30] W. I. F. David, R. M. Ibberson, and J. C. Matthewman (unpublished).

[31] V. F. Sears, Neutron News **3**, 26 (1992).

[32] K. Otzschi, A. Hayashi, and Y. Ueda, Physica C **235**, 839 (1994).

[33] Y. Tokura, J. B. Torrance, F. C. Huang, and A. I. Nazzal, Phys. Rev. B **38**, 7156 (1988).

[34] R. G. Buckley, D. M. Pooke, J. L. Tallon, M. R. Pressland, N. E. Flower, M. P. Staines, H. L. Johnson, M. Meylan, G. V. M. Williams, and M. Bowden, Physica C **174**, 383 (1991).

[35] X. Sishen, Y. Cuiying, W. Xiaojing, C. Guangcan, F. Hanje, C. Wei, Z. Yuqing, Z. Zhongzian, Y. Qiansheng, C. Genghua, L. Jinkjui, and L. Fanghua, Phys. Rev. B **36**, 2311 (1987).

[36] H. Schwer, E. Kaldis, J. Karpinski, and C. Rossel, J. Solid State Chem. **111**, 96 (1994).

[37] C. A. Hijar, C. L. Stern, K. R. Poeppelmeier, K. Rogacki, Z. Chen, and B. Dabrowski, Physica C **252**, 13 (1995).

[38] V. A. Trounov, T. Y. Kaganovich, P. Fischer, E. Kaldis, J. Karpinski, and E. Jikel, Physica C **227**, 285 (1994).

[39] P. Fischer, E. Kaldis, J. Karpinski, S. Rusiecki, E. Jilek, V. Trounov, and A. W. Hewat, Physica C **205**, 259 (1993).

[40] X. Zhang, Physica C **222**, 227 (1994).

[41] I. Mangelschots, M. Mali, J. Roos, H. Zimmermann, D. Brinkmann, S. Rusiecki, J. Karpinski, E. Kaldis, and E. Jilek, Physica C **172**, 57 (1990).

[42] I. Mangelschots, M. Mali, J. Roos, H. Zimmermann, D. Brinkmann, J. Karpinski, E. Kaldis, and S. Rusiecki, J. Less-Common Met. **164**, 78 (1990).

[43] M. Knupfer, N. Nücker, M. Alexander, H. Romberg, P. Adelmann, J. Fink, J. Karpinski, E. Kaldis, S. Rusiecki, and E. Jilek, Physica C **182**, 62 (1991).

[44] G. Triscone, M. Francois, J-Y. Genoud, T. Graf, A. Junod, C. Opagiste, and J. Muller, J. Alloys Compd. **196**, 235 (1993).

[45] H. Zhang and H. Saito, Phys. Rev. Lett. **70**, 1697 (1993).

[46] J. M. S. Skakle, A. Templeton, E. E. Lachowski, and A. R. West, Physica C **260**, 137 (1996).